Journal of Modern Optics

ISSN: 0950-0340 (Print) 1362-3044 (Online) Journal homepage: https://www.tandfonline.com/loi/tmop20

Single facet semiconductor laser with deep etched V-notch reflectors integrated with an active multimode interference reflector

Mohamad Dernaika, Ludovic Caro, Niall P. Kelly & Frank H. Peters

To cite this article: Mohamad Dernaika, Ludovic Caro, Niall P. Kelly & Frank H. Peters (2017) Single facet semiconductor laser with deep etched V-notch reflectors integrated with an active multimode interference reflector, Journal of Modern Optics, 64:19, 1941-1946, DOI: 10.1080/09500340.2017.1327621

To link to this article: https://doi.org/10.1080/09500340.2017.1327621

JOURNAL OF MODERN OPTICS, 2017
VOL. 64, NO. 19, 1941–1946
https://doi.org/10.1080/09500340.2017.1327621

Taylor & Francis
Taylor & Francis Group

Single facet semiconductor laser with deep etched V-notch reflectors integrated with an active multimode interference reflector

Mohamad Dernaika[a,b], Ludovic Caro[a,c], Niall P. Kelly[a,c] and Frank H. Peters[a,c]

[a]Integrated Photonics Group, Tyndall National Institute, Cork, Ireland; [b]Electrical and Electronic Engineering Department, University College Cork, Cork, Ireland; [c]Physics Department, University College Cork, Cork, Ireland

ABSTRACT
A single mode laser based on novel deep etched V-notch reflectors is presented in this paper. The reported device has a stable single mode operation and a side mode suppression ratio of 37 dB. The laser is widely tunable and it can be fine-tuned. Moreover, the laser cavity is monolithically integrated with an active multimode interference reflector, and has a total length of 860 μm.

ARTICLE HISTORY
Received 23 March 2017
Accepted 23 April 2017

KEYWORDS
Semiconductor laser; single mode laser; InP

1. Introduction

Single mode semiconductor lasers using coupled cavities (*1*) and higher order gratings (*2*) have attracted a lot of research interest as potential candidates to compete with Bragg grating-based lasers (*3*). The higher order grating-based slotted Fabry Perot (SFP) laser for example can be widely tunable to match the ITU grid and thermally tuned to provide reliable small wavelength steps for applications such as dense wavelength division multiplexing (DWDM) (*4*). They also have one significant advantage over distributed Bragg reflector (DBR) and distributed feedback (DFB) lasers: they do not require epitaxial regrowth or high resolution processes such as electron beam lithography (e-beam) (*5*) that significantly increase the process time and cost.

SFP lasers have been extensively investigated. Using standard UV lithography, SFP lasers provide a tunable output with a high side mode suppression ratio (SMSR) and narrow linewidth (*6*). The reflections from the slots provide optical feedback. Thus, the free spectral range (FSR) can be defined based on the slot spacing and therefore acts as a single mode selector. The slots can be also used as an active mirror, in a configuration similar to sampled grating (SG) DBR lasers in order to provide optical feedback and eliminate the need of a facet (*7*). These designs have proven to be effective and relatively simple in comparison with DFB and DBR lasers.

Slot depth is a critical parameter that contributes to the laser performance (*8*). A slight depth variation will affect both the slot reflection and loss. Using plasma etching, reaching the same depth at each fabrication run or across the same chip is not always achievable. As a result, it is challenging to ensure that the overall laser performance it repeatable between fabrication runs. In order to provide a better depth consistency, a combination of dry etch and wet chemical etch steps can be used (*9*). However, using the wet chemical etch will increase the fabrication complexity due to the influence of crystal orientation on chemical etching of InP (*10*–*12*).

In this paper, we present a compact, tunable and single mode laser based on V-notch reflector structure. The V-notch is deeply etched past the active region. It is therefore not depth sensitive and does not require wet chemical etching for accurate depth control. The reported laser has a simple fabrication process, exhibits an SMSR of 37 dB and is tunable. As an addition, one of the facets is replaced with a monolithically integrated multi-mode interference reflector (MIR) (*13*). An illustration of the device is shown in Figure 1.

2. Device design and fabrication

The schematic in Figure 1 shows the two section laser design, along with Scanning electron microscope (SEM) images of the V-notch reflector on the top left and MIR on the top right. The total length of the cavity is 880 μm. The laser consists of two sections (A and B) separated by an angled slot to provide electrical isolation between the two contact pads.

Section A of the laser has a length of 460 μm and it comprises of an MIR and a waveguide section. MIRs

CONTACT Mohamad Dernaika mohamad.dernaika@tyndall.ie

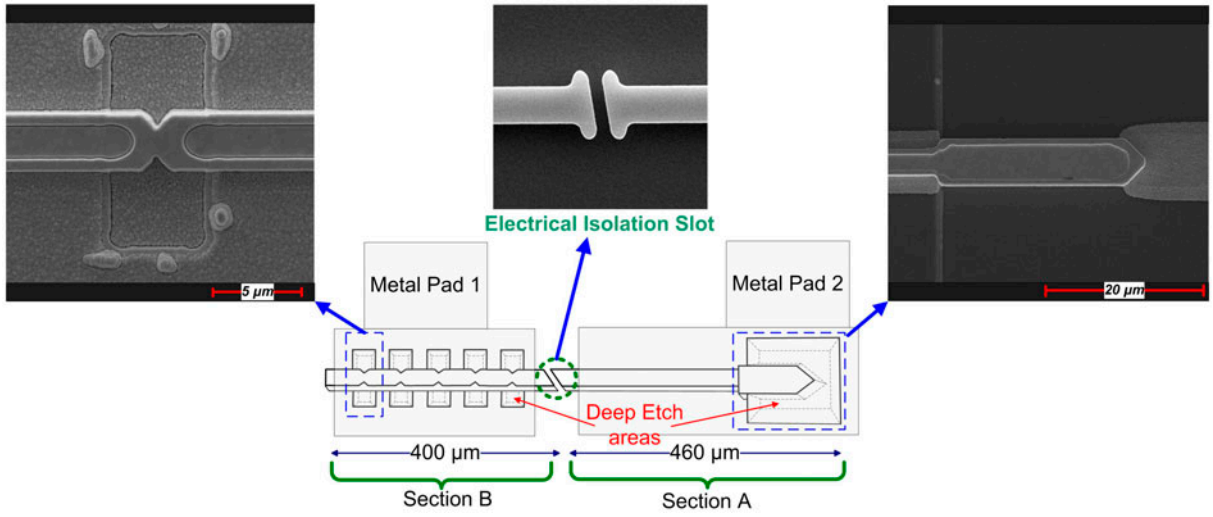

Figure 1. Illustration of the two-section Laser cavity design along with SEM images of the V-notch, isolation slot and MIR.

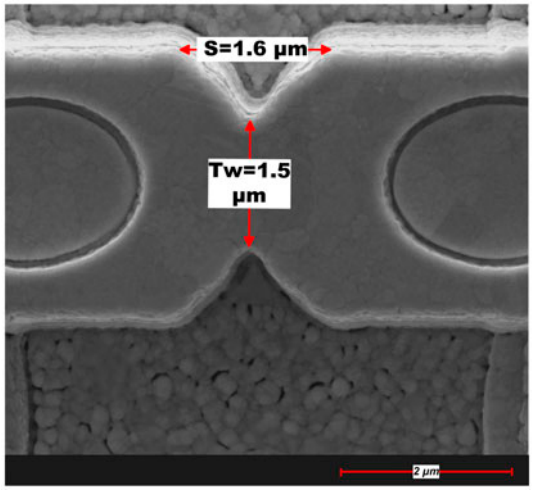

Figure 2. SEM image of the V-notch with dimensions.

have been recently developed to allow mid-chip integration of mirrors to replace cleaved facets (*14*, *15*). This makes them a valuable integration tool and a potentially important building block for InP-based Photonic-integrated circuits (PICs). The active MIR has a length of 25 μm and width of 5 μm, and uses the same epitaxy as the laser, thus avoiding the need for epitaxial regrowth. The structure uses a deep etch that extends through the active region and lower cladding to ensure a strong light confinement which maximizes the reflected power back into the cavity. The design of the MIR is similar to a 1×2 multimode interference coupler terminating with 45° angles. The incident light is reflected on the angled facet and back into the waveguide due to total internal reflection. The active MIR design and fabrication process is similar to the reflector reported in (*16*). Although theoretically the MIR should reflect back 100% of the light, it has been shown that it suffers from some loss. Nonetheless, when optimized, it is still a convenient solution to replace cleaved facets because it allows a flexible positioning of the laser on the chip.

Section B of the laser consists of the wavelength selective mirror. This section is 400 μm long and contains five 80 μm equally spaced V-shaped partial reflectors. The reflected light resonates between the V-notch structures and with both MIR and the cleaved facet creating a coupled cavity laser. The reflectors are deeply etched through the quantum wells in order to ensure effective reflections. The reflectors were etched in the same process as the MIR, so no additional processing was required.

Figure 2 shows a close up SEM image of the reflector with the dimensions of the structure. The original width of the waveguide is 2.5 μm. Tw is the tapered width 1.2 μm and S represents the taper length needed to form the V-notch reflector. Moreover, it is possible to include in the same cavity different V-notch reflectors with different parameters without adding any steps because S and Tw are defined in the same lithography step of the ridge. The flexibility can be considered as an advantage compared to slots, where the etch depth plays a critical role in controlling the reflections and loss. Due the intrinsic design of the slot, it is not possible to include slots with different depths on the same cavity without additional fabrication steps.

To analyse the reflections and losses of the V-notch, a 3D module of the epitaxial layers with a single V-notch was simulated using a commercial software: ModePROP from RSoft. The software employs a widely used bi-directional eigenmode expansion method (EEM) approach that takes all reflections into account. Figure 3 shows the reflection, loss and transmission for the slot and for the V-notch with a ridge high of 1.8 μm. Figure 3(a) shows the simulation of the slot and

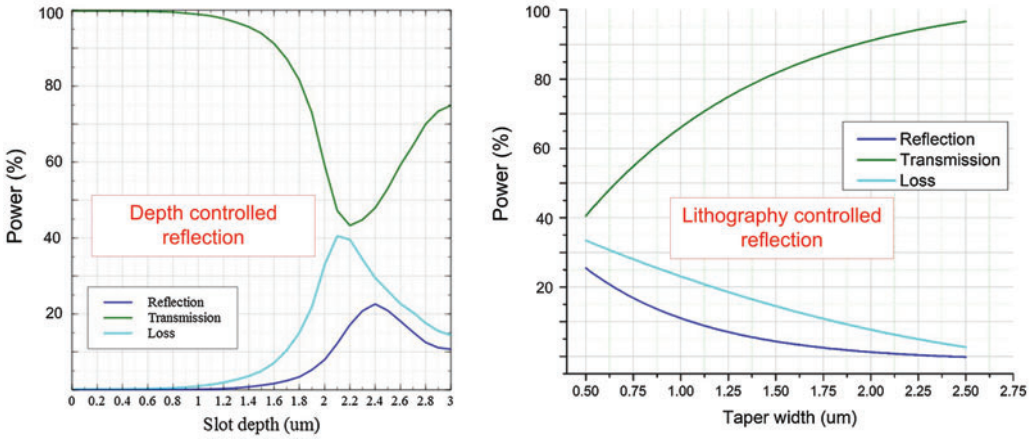

Figure 3. Simulation results of reflection, loss and transmission for (a) slot depth variation, (b) V-notch taper width variation.

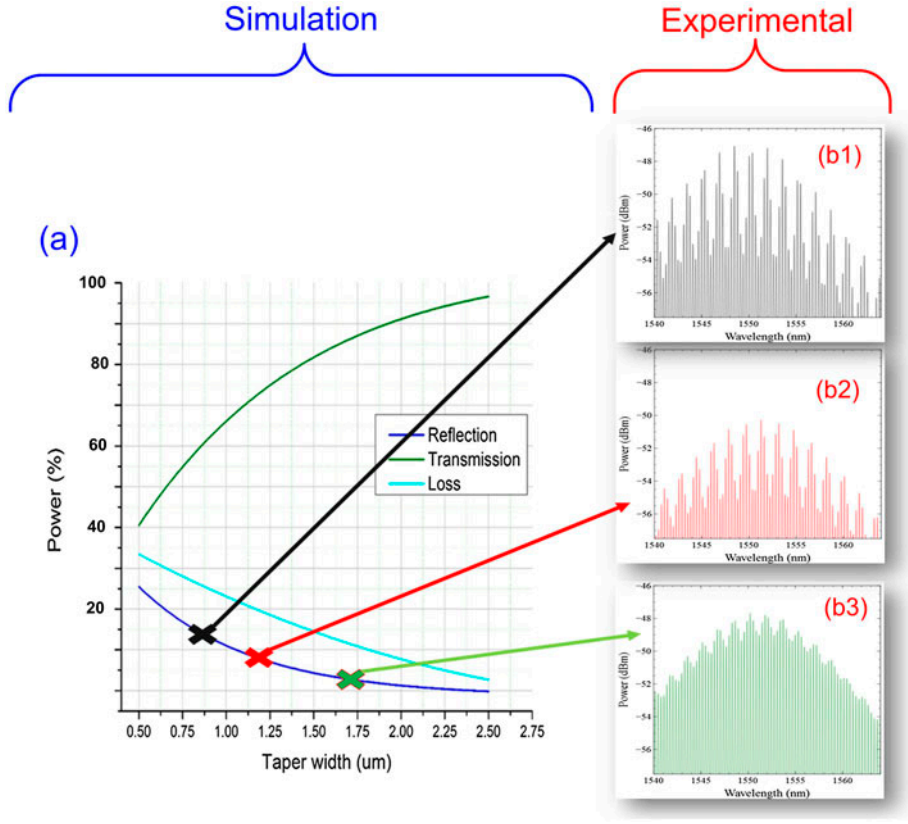

Figure 4. (a) V-notch simulation results showing reflection (blue), loss (cyan) and transmission (green), (b1) to (b3) experimental spectrum at various V-notch taper width.

demonstrates how the reflection is depth controlled. Figure 3(b) shows the V-notch simulation and how the reflection is lithographically controlled by varying the taper width Tw from 0.5 to 2.5 μm.

In Figure 3(b), the simulation shows a pseudo-linear relation between loss and reflection governed by the taper width. An increase in reflection will increase loss and consequently reduce the transmission. A trade-off between reflection and loss is observed.

To verify the operation of the V-notch reflectors, three Fabry Perot (FP) laser cavities were fabricated. All three FP lasers had the same length of 1.1 mm but each included a single V-notch with a different taper width Tw. The simulation graph in Figure 4(a) shows the reflection curve (blue line), and Figure 4(b1),(b2) and (b3) shows the experimental spectrum data from V-notch with taper widths 0.75, 1.2 and 1.7 μm, respectively. The periodic modulation depth caused from the V-notch increases

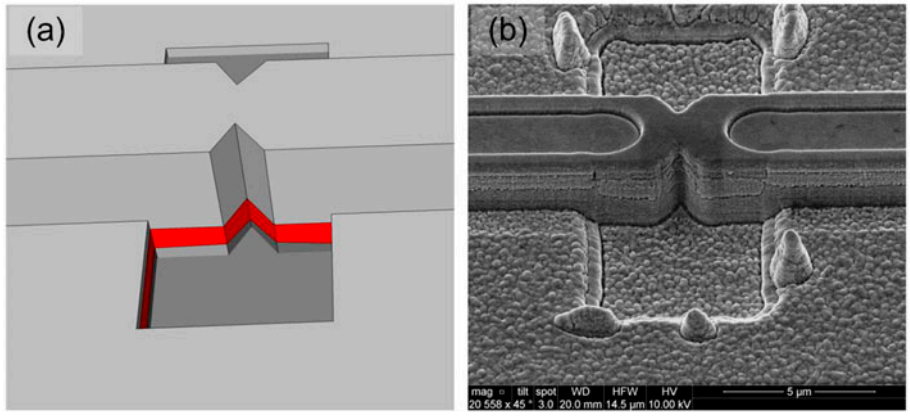

Figure 5. (a) Illustration of the etch depth, (b) SEM image showing the deep etch region.

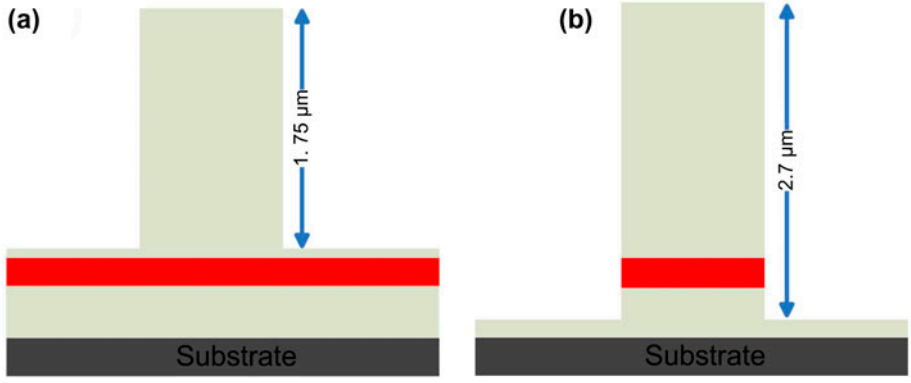

Figure 6. (a) Shallow ridge, (b) Deep ridge.

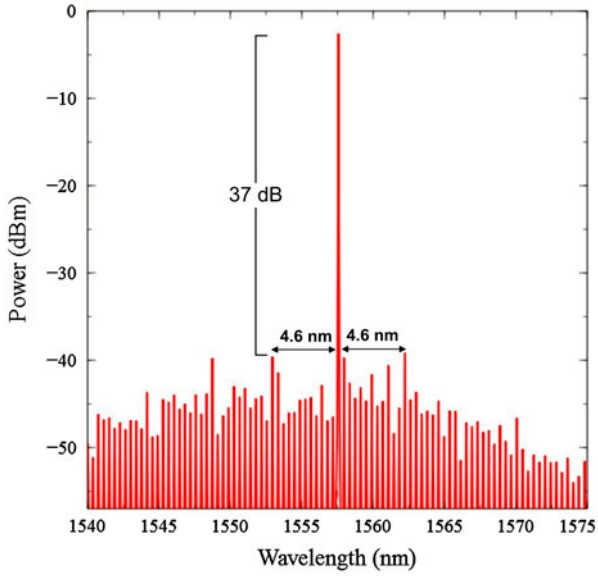

Figure 7. Laser output with 37 dB SMSR.

with the decrease in the taper width. The experimental data agree well with the simulation, which suggests that the reflection strength increases with a decrease in taper width. The V-notch is not depth sensitive; however, to obtain a strong reflection, the structure was deeply etched through the active region and into the lower cladding. Due to the nature of the V-notch, smooth side walls are very important to reduce scattering loss and ensure the light is reflected back into the waveguide. Moreover, Figure 4 shows a trade-off between reflection and transmission, which means the V-notch number and dimension should be taken into consideration when designing a cavity. The large number or highly reflective V-notch structures with a relatively short gain section limits the laser linewidth and output power due to cavity losses. Figure 5(a) shows an illustration of the design of the deeply etched V-shaped structures. The red colour represents the active region, where the ridge and the cladding layers are in grey. Figure 5(b) shows a side view SEM image that includes the deep etch ridge. The opening on the top of the ridge is the oxide window for metal contact layer. The roughness on the floor is also due to the metal deposition.

The entire device was fabricated without any epitaxial regrowth or high resolution lithography. The active layers of the wafer comprise 5×6 nm AlInGaAs strained quantum wells sandwiched between 610 nm barriers. The top cladding directly above the quantum wells consists of

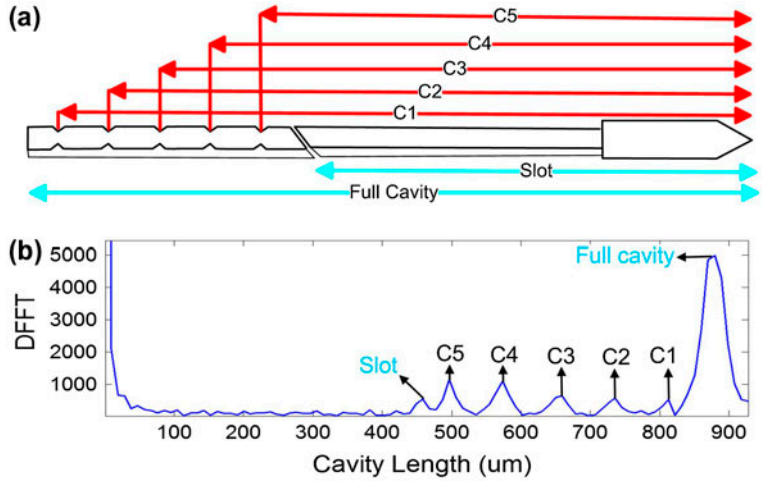

Figure 8. (a) Laser design with highlighted cavities, (b) FFT analysis.

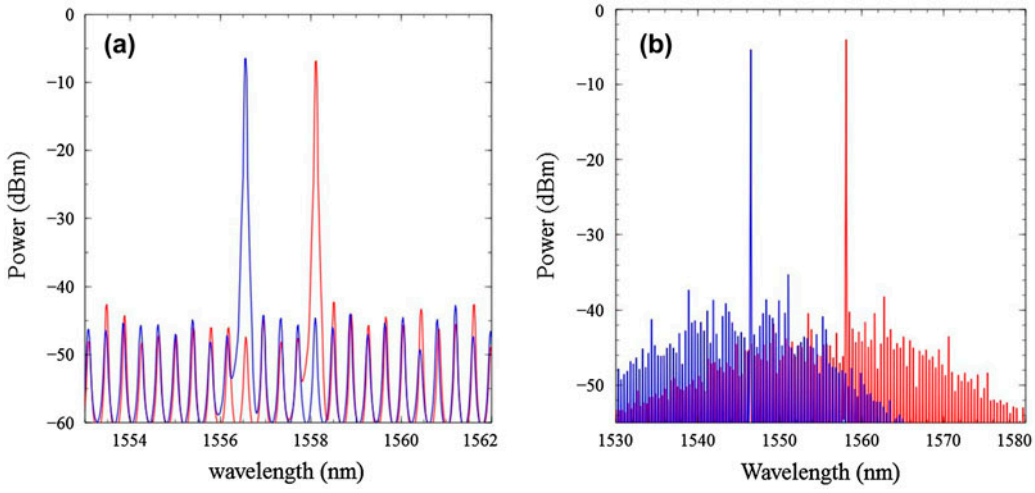

Figure 9. (a) Fine tuning, (b) wide tuning.

a 20 nm GaInAsP etch stop layer and 1580 nm InP layer deposited under a 50 nm GaInAsP and 200 nm GaInAs metal contact layer. The total thickness of the cladding region excluding the etch stop layer is approximately 1.81 μm. The fabricated laser has two different etched regions as shown in Figure 6.

A shallow etch region with a height of 1.75 μm was used to define the ridge and the isolation slot depth, whereas the deep etch region was used for the MIR and the V-notch reflectors as shown in Figure 1.

3. Results and discussion

The laser was mounted on a brass chuck that was temperature controlled using a thermal electric cooler (TEC). A lensed fibre was used on the cleaved facet side to collect the light and inspect the spectrum and optical power. Two separate current sources were utilized to inject current into the laser. Figure 7 shows the optical spectrum of the laser, with a single mode emission at 1557.5 nm and an SMSR of 37 dB. The free spectral range of the V-shaped reflectors can be visibly distinguished on the lasing output. The measured spacing of 4.6 nm between the main mode and the adjacent side modes corresponds to an 80 μm cavity length which is the spacing between the V-notch structures.

By employing a fast Fourier transform (FFT) algorithm, it was possible to extract the effective lengths of the coupled cavities from the optical spectrum of the laser at threshold. As Figure 8 shows, the FFT analysis of the optical spectrum agreed with the effective physical length of the coupled cavities.

The FFT analysis shows the actual cavities' effective length based on the FSR of the laser modes. The five peaks in Figure 8(b) graph labelled from C1 to C5 correspond to the physical lengths shown on the laser design

in Figure 8(a). The large reflection peak on the right of C1 represents the laser full cavity length extending from the MIR to the cleaved facet, whereas the small peak just before C5 is a small unintentional reflection caused from the isolation slot. The single mode output can be continuously tuned thermally with small changes in applied bias, or it can be discretely tuned using larger bias steps, which result in mode hopping. Figure 9 shows the two tuning options. The thermal tuning led to a red shift around 20 pm/1 mA covering 1.5 nm before hopping to the next mode as shown in Figure 9(a). Figure 9(b) shows the laser wide tuning range that can cover around 12.5 nm.

4. Conclusion

The laser reported in this paper has the advantage of being both compact and straightforward to fabricate, and is monolithically integrated with an MIR. The V-notch reflectors offer the benefit of being lithography controlled, and they do not require high resolution lithography such as e-beam or advanced fabrication methods. It is therefore possible to include different V-notch reflectors with different dimensions without any additional fabrication steps. The laser achieved a stable thermal tuning of 20 pm/mA over approximately 1.5 nm, and it exhibits an SMSR of 37 dB.

Disclosure statement

No potential conflict of interest was reported by the authors.

Funding

This work was supported by the Science Foundation Ireland [grant number SFI 13/IA/1960], [grant number 12/RC/2276 (I-PIC)].

References

(1) Zhang, S.; Meng, J.; Guo, S.; Wang, L.; He, J.J. Simple and Compact V-cavity Semiconductor Laser with 50 × 100 GHz Wavelength Tuning. *Opt. Express* **2013,** *21* (11), 13564–13571.

(2) Li, Y.; Xi, Y.; Li, X.; Huang, W.P. Design and Analysis of Single Mode Fabry-Perot Lasers with High Speed Modulation Capability. *Opt. Express* **2011,** *19* (13), 12131–12140.

(3) Golka, S.; Austerer, M.; Pflügl, C.; Andrews, A.M.; Roch, T.; Schrenk, W.; Strasser, G. GaAs/AlGaAs Quantum Cascade Lasers with Dry Etched Semiconductor-Air Bragg Reflectors. *J. Mod. Opt.* **2005,** *52* (16), 2303–2308.

(4) Ramaswamy, P.; Roycroft, B.; O'Callaghan, J.; Janer, C.; Peters, F.; Corbett, B. Wavelength Agile Slotted Fabry-Pérot Lasers. In *2014 International Semiconductor Laser Conference (ISLC)*; IEEE, Palma de Mallorca, Spain, 2014; pp 102–103.

(5) Verheijen, M. E-beam Lithography for Digital Holograms. *J. Mod. Opt.* **1993,** *40* (4), 711–721.

(6) Kelly, B.; Phelan, R.; Jones, D.; Herbert, C.; O'Carroll, J.; Rensing, M.; Wendelboe, J.; Watts, C.; Kaszubowska, A.; Anandarajah, P.; Guignard, C.; Barry, L.P.; O'Gorman, J. Discrete Mode Laser Diodes with very Narrow Linewidth Emission. *Electron. Lett.* **2007,** *43* (23), 1282–1284.

(7) Byrne, D.C.; Engelstaedter, J.P.; Guo, W.H.; Lu, Q.Y.; Corbett, B.; Roycroft, B.; O'Callaghan, J.; Peters, F.; Donegan, J.F. Discretely Tunable Semiconductor Lasers Suitable for Photonic Integration. *IEEE J. Sel. Top. Quantum Electron.* **2009,** *15* (3), 482–487.

(8) Lu, Q.; Guo, W.; Phelan, R.; Byrne, D.; Donegan, J.; Lambkin, P.; Corbett, B. Analysis of Slot Characteristics in Slotted Single-mode Semiconductor Lasers using the 2-D Scattering Matrix Method. *IEEE Photonics Technol. Lett.* **2006,** *18* (24), 2605–2607.

(9) Phelan, R.; Guo, W.H.; Lu, Q.; Byrne, D.; Roycroft, B.; Lambkin, P.; Corbett, B.; Smyth, F.; Barry, L.P.; Kelly, B.; O'Gorman, J.; Donegan, J.F. A Novel Two-section tunable Discrete Mode Fabry-Perot Laser Exhibiting Nanosecond Wavelength Switching. *IEEE J. Quantum Electron.* **2008,** *44* (4), 331–337.

(10) Kelly, J.J.; Philipsen, H.G. Anisotropy in the Wet-etching of Semiconductors. *Curr. Opin. Solid State Mater. Sci.* **2005,** *9* (1), 84–90.

(11) Siwak, N.; Fan, X.; Ghodssi, R. Fabrication Challenges for Indium Phosphide Microsystems. *J. Micromechan. Microeng.* **2015,** *25* (4), 043001.

(12) Dernaika, M.; Caro, L.; Kelly, N.; Alexander, J.; Dubois, F.; Morrissey, P.; Peters, F. Deeply Etched Inner-cavity Pit Reflector. *IEEE Photonics J.* **2017,** *9* (1), 1–8.

(13) Kleijn, E.; Smit, M.K.; Leijtens, X.J. Multimode Interference Reflectors: A New Class of Components for Photonic Integrated Circuits. *J. Lightwave Technol.* **2013,** *31* (18), 3055–3063.

(14) Zhao, J.; Kleijn, E.; Smit, M.K.; Williams, P.J.; Knight, I.; Wale, M.J.; Leijtens, X.J. Novel Lasers using Multimode Interference Reflector. In *2011 ICO International Conference on Information Photonics (IP)*; IEEE, Ottawa, ON, Canada, 2011; pp 1–2.

(15) Xu, L.; Leijtens, X.; Docter, B.; De Vries, T.; Smalbrugge, E.; Karouta, F.; Smit, M.K. MMI-reflector: A Novel On-chip Reflector for Photonic Integrated Circuits. In *35th European Conference on Optical Communication, 2009. ECOC'09*; IEEE, Vienna, Austria, 2009; pp 1–2.

(16) Morrissey, P.E.; Kelly, N.; Dernaika, M.; Caro, L.; Yang, H.; Peters, F.H. Coupled Cavity Single-mode Laser Based on Regrowth-free Integrated MMI Reflectors. *IEEE Photonics Technol. Lett.* **2016,** *128* (12), 1313–1316.